Definition of percolation thresholds on self-affine surfaces

Marrink, S.J.; Paterson, Lincoln; Knackstedt, Mark A.

Published in:
Physica A: Statistical Mechanics and its Applications

DOI:
10.1016/S0378-4371(99)00608-1

Publication date:
2000

ELSEVIER

Physica A 280 (2000) 207–214

PHYSICA A

www.elsevier.com/locate/physa

Definition of percolation thresholds on self-affine surfaces

S.J. Marrink[a], Lincoln Paterson[b], Mark A. Knackstedt[a,c,*]

[a] *Department of Applied Mathematics, Research School of Physical Sciences and Engineering, Australian National University, Canberra ACT 0200, Australia*

[b] *Australian Petroleum Cooperative Research Centre, CSIRO Division of Petroleum Resources, PO Box 3000, Glen Waverley, Vic 3150, Australia*

[c] *Australian Petroleum Cooperative Research Centre, University of New South Wales, Sydney, NSW 2052, Australia*

Received 28 January 1999

Abstract

We study the percolation transition on a two-dimensional substrate with long-range self-affine correlations. We find that the position of the percolation threshold on a correlated lattice is no longer unique and depends on the spanning rule employed. Numerical results are provided for spanning across the lattice in specified (horizontal or vertical), either or both directions.

Keywords: Percolation; Fractal Brownian motion; Porous sedimentary rocks

1. Introduction

The study of multiphase flow phenomena in sedimentary rocks has presented many challenges to the physics community. Relevant applications are found in transport of non-aqueous contaminants in groundwater and the production of oil and gas from sedimentary reservoirs. Important contributions to understanding multiphase flow observations in porous media and rock have been made using percolation theory [1,2]. In particular, percolation theory has been used to explain residual or trapped fluids in a two-fluid displacement, where the amount of residual fluid is analogous to the percolation threshold p_c.

In most applications of percolation theory, spatial disorder has been assumed to be uncorrelated, but it has become evident that long-range correlations exist in many

* Corresponding author. Fax: +61-2 6249 0732.

0378-4371/00/$ - see front matter
PII: S0378-4371(00)00608-1

porous sedimentary rocks. Studies have shown that long-range correlations in properties exist from the kilometer scale to the pore scale [3–9]. To describe the correlations, fractional Brownian motion (fBm) was introduced by Hewett [3] as a model for the underlying reservoir heterogeneity. The recognition that natural porous media frequently have long-range spatial correlations in their properties has encouraged studies of percolation in correlated property maps generated by fBm [10–14].

The generation of percolation quantities through numerical Monte-Carlo simulation requires the use of finite lattices and extrapolation toward infinity. However, when long-range correlations are introduced, new interpretation is required because various quantities that converge with lattice size on uncorrelated networks no longer do so on correlated networks. In ordinary percolation on an uncorrelated lattice there is a *unique* value of p_c, the point at which a transition in the topological structure of the network from a macroscopically disconnected structure to a connected one occurs. In this paper we show that the percolation threshold on correlated lattices is dependent on the spanning rule employed and can therefore be interpreted differently for different applications. In flow in porous media, applications generally involve flow from a point or distributed source to a sink. Thus the concept of spanning between the source and the sink is important. This contrasts with a percolation threshold definition based on an incipient infinite cluster. On uncorrelated lattices, these subtle details are insignificant. However, on correlated lattices this is no longer the case.

Different spanning rules on uncorrelated networks were considered by Reynolds et al. [15] when studying renormalization to obtain critical parameters at the percolation threshold. They defined rules on a square lattice where rule $\Re_0$ is the probability of spanning *either* horizontally or vertically or both, $\Re_1$ is the probability of spanning in a *fixed* direction (e.g. horizontally), and $\Re_2$ is the probability of spanning *both* horizontally and vertically. On finite lattices these rules give different results, but they converge as the lattice size approaches infinity. The probabilities are not independent, with $\Re_0 = 2\Re_1 - \Re_2$.

A number of important observations regarding percolation on self-affine surfaces have been made by Schmittbuhl et al. [10]. They considered renormalization on a self-affine hierarchical construction as well as performing numerical simulations on self-affine lattices generated using a mid-point displacement algorithm. They established that the percolation process, even on an infinite lattice, will behave as if the system was finite in the absence of correlation. Their numerical simulations were based on an interpretation equivalent to $\Re_1$ without considering rules $\Re_0$ and $\Re_2$. Their conclusion regarding finite behaviour would imply, however, that $\Re_0$ and $\Re_2$ will converge to distinctly different numerical values. In this paper we perform numerical simulations to verify that this is indeed the case.

Percolation thresholds have also been estimated by Du et al. [11] using a mid-point displacement algorithm to generate approximate fractional Brownian motion. Examination of their results shows that they used the $\Re_0$ interpretation for the percolation threshold. Hence Du et al. [11] and Schmittbuhl et al. [10] obtain contrasting values, which can be explained when the various spanning rules are considered.

2. Algorithms

2.1. Fractional Brownian motion

Fractional Brownian motion is a way of introducing long-range correlations into a discrete stochastic property map $V(r)$ where r is the spatial coordinate [16,17]. The average variance of the increments ΔV of fractional Brownian motion scales with distance between points Δr as a power law

$$\Delta V \propto \Delta r^H, \tag{1}$$

where H is known as the Hurst parameter, $0 < H < 1$. For $H > 0.5$, positive increments tend to be followed by positive increments (persistence), while for $H < 0.5$ positive increments tend to be followed by negative increments (antipersistence).

A variety of methods exist for generating approximate fractional Brownian motion, and published algorithms are available [18,19]. Of the methods listed here, the mid-point displacement methods are the fastest, but the generated maps have non-stationary increments when $H \neq 0.5$. This means they are not true fBm, but are nevertheless statistically self-affine. Fourier methods are also reasonably fast, but the chief difficulty is the restriction of periodic boundaries and aliasing errors. Selecting small regions from larger generated maps helps overcome these problems, but at significant computational and memory expense. The turning bands method can generate high-quality fBm [20], but artifacts stem from the finite number of lines and the discretization along these lines. These artifacts can be overcome by using many lines and points, but this makes the method particularly slow.

Like Du et al. [11] and Schmittbuhl et al. [10], we elected to use the mid-point method for its computational speed and the ability to perform large numbers of realizations and obtain good statistics. Some comparisons were performed with the three methods on smaller lattices: while the numerical results had differences, the qualitative behavior was the same. We did not consider the effect of lacunarity.

We added a factor $1-(2-2^H)^{0.5}$ to the variances of the displacements in Saupe's 2D pseudo-code [18]. This corrects an inconsistency in the first step of the algorithm. It only affects the first step as the factor is applied recursively. Also problematic to midpoint methods is the choice of the initial value of the corner points. In Saupe's algorithm [18], the four corner points are initialized independently as Gaussian random variables with zero mean and constant standard deviation. To be self-affine the four initial corner points are not independent. Hence, we set one corner to zero, initialized the two adjacent corners with Gaussian random variables, then extrapolated the fourth corner point from the other three with a scaling factor of $\sqrt{2}$. Schmittbuhl et al. [10] used a different approach with periodic boundaries and equal corner points. We performed a number of tests and concluded that these differences create only minor differences in the results, and do not change any qualitative results.

2.2. Spanning rules

In traditional site percolation studies the percolation threshold p_c is defined as the value of the minimum concentration p of sites chosen at random to form an infinite cluster with probability 1. Equivalently one can search for the existence of a percolation network of filled sites. A common way of choosing whether sites are filled or not involves attributing to each site x a number picked from a random distribution $\phi(x)$ and deciding that a site x_0 is present if $\phi(x_0)$ is less than a threshold x_c so that $\int_{-\infty}^{x_c} \phi(x)\,\mathrm{d}x = p$. We follow this procedure but use fBm to define the statistically self-affine field $\phi(x)$ on the sites of the lattice. The values of $\phi(x)$ can be interpreted as heights on a discretised landscape. All sites below a certain height $\phi(x_c)$ are considered covered and one determines at what value of $p = p_c$ the covered regions of the lattice span.

To detect spanning we used the Hoshen–Kopelman algorithm [23,24]. A faster hull-generating walk method has been previously used by Ziff [21] and Grassberger [25]. However, in our case, the generation of the fBm correlations becomes a time limiting step rather than the choice of algorithm to detect spanning, hence there is less incentive to use the fast hull-generating walks. This is more so for fBm algorithms that are slower than the mid-point method. Furthermore, hull-generating walks do not easily extend to three dimensions [22].

We consider three definitions of the percolation threshold on an $L \times L$ square network. The first definition p_c^{eith} is when *either* of the two opposite faces (left–right or top–bottom) of a square region become connected; whichever occurs first. The second measurement p_c^{both} is when we require *both* faces to be connected, top–bottom as well as left–right. A third measurement p_c^{spec} is provided when we allow connections in a *specified* direction only, say top–bottom. These three definitions are related to the spanning rules $\mathfrak{R}_0$, $\mathfrak{R}_1$ and $\mathfrak{R}_2$ defined by Reynolds et al. [15], with the subtle distinction described above in that we look at the mean fraction of sites occupied when spanning occurs. The percolation threshold obtained according to the third definition will be the averaged value of the two other definitions [15,22].

As we show below, percolation thresholds for individual correlated lattices scatter widely, and therefore one needs to average over many independently generated realizations in order to obtain good accuracy. This creates particular problems with execution time on large correlated lattices, especially when H is large.

3. Results

Results of simulations on uncorrelated lattices are shown in Table 1, results from correlated lattices are shown in Tables 2–4 for values of the Hurst exponent, $H = 0.2, 0.5$, and 0.8. The number of independent realizations are shown with the data. An example of the spread of individual realizations is shown in Fig. 1 for a network size of 128×128.

Table 1
Fraction of sites occupied when spanning first occurs in *either*, *specified*, or *both* directions. Values are mean ± one standard deviation on an uncorrelated random lattice

L	Realizations	Either	Specified	Both
32	70 000	0.576 ± 0.036	0.593 ± 0.039	0.610 ± 0.035
64	70 000	0.583 ± 0.021	0.593 ± 0.023	0.603 ± 0.021
128	30 000	0.587 ± 0.013	0.593 ± 0.014	0.599 ± 0.013
256	10 000	0.589 ± 0.008	0.593 ± 0.008	0.596 ± 0.007
512	6 000	0.591 ± 0.004	0.593 ± 0.005	0.595 ± 0.004
1024	3 000	0.5914 ± 0.0027	0.5927 ± 0.0030	0.5940 ± 0.0026
2048	3 000	0.5920 ± 0.0016	0.5927 ± 0.0018	0.5935 ± 0.0016

Table 2
Correlated lattice thresholds, $H = 0.2$

L	Realizations	Either	Specified	Both
32	70 000	0.465 ± 0.096	0.537 ± 0.117	0.609 ± 0.090
64	70 000	0.461 ± 0.094	0.532 ± 0.115	0.604 ± 0.089
128	30 000	0.457 ± 0.093	0.528 ± 0.115	0.599 ± 0.089
256	30 000	0.454 ± 0.093	0.524 ± 0.115	0.595 ± 0.089
512	20 000	0.450 ± 0.092	0.521 ± 0.114	0.591 ± 0.089

Table 3
Correlated lattice thresholds, $H = 0.5$

L	Realizations	Either	Specified	Both
32	70 000	0.427 ± 0.113	0.521 ± 0.147	0.615 ± 0.108
64	70 000	0.420 ± 0.113	0.515 ± 0.147	0.610 ± 0.110
128	30 000	0.416 ± 0.112	0.511 ± 0.147	0.607 ± 0.111
256	30 000	0.412 ± 0.112	0.508 ± 0.147	0.604 ± 0.112
512	20 000	0.412 ± 0.111	0.507 ± 0.147	0.602 ± 0.112
1024	10 000	0.407 ± 0.112	0.505 ± 0.147	0.602 ± 0.112

Table 4
Correlated lattice thresholds, $H = 0.8$

L	Realizations	Either	Specified	Both
32	70 000	0.391 ± 0.131	0.509 ± 0.176	0.627 ± 0.128
64	70 000	0.387 ± 0.133	0.506 ± 0.177	0.624 ± 0.130
128	30 000	0.384 ± 0.132	0.504 ± 0.177	0.623 ± 0.130
256	30 000	0.383 ± 0.133	0.502 ± 0.177	0.621 ± 0.130
512	20 000	0.382 ± 0.131	0.501 ± 0.177	0.621 ± 0.131

From the results we were able to make the following observations. First, we observed that the percolation thresholds in fBm-correlated lattices are strongly dependent on the definition used. Percolation in *either* direction is observed much earlier than in *both* directions. On the contrary, for uncorrelated lattices, the simulated difference between

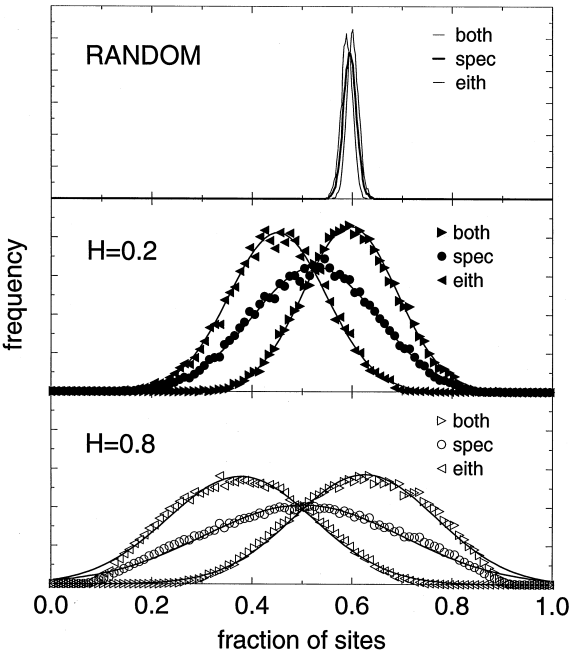

Fig. 1. Distributions of fractions of sites filled when spanning first occurs (both, either or specified directions). Results were obtained from averaging over 30 000 realizations of size 128×128, for uncorrelated lattice, fBm with $H = 0.2$, and fBm with $H = 0.8$. In both figures we show the narrow distribution obtained for an uncorrelated lattice.

the definitions is insignificant. The difference between p_c^{both} and p_c^{eith} increases as the persistence of the correlation H increases.

Second, the threshold for percolation in a specified direction p_c^{spec}, is close to the value $p = 0.5$. For uncorrelated square lattices, the percolation threshold has been estimated by others as $p_c \simeq 0.5927$ [21,26]. It is not clear why the site percolation threshold on the correlated square grid corresponds to the threshold for more highly coordinated lattices (e.g., triangular lattice). For percolation in both directions p_c^{both} increases with H and conversely p_c^{either} decreases with H.

A third generally observed feature for fBm correlated lattices is that the variation in the spanning threshold between realizations is very wide. Greater variance is obtained for spanning in a specified direction than for either or both directions. Consistent with others [10–12,27] the standard deviations of the percolation threshold distribution appear to remains finite as $L \to \infty$. For small H the distributions give a reasonable fit to a Gaussian distribution, while for larger H, the distributions show strong deviations from Gaussian behavior at the tails.[1] Standard deviations increase with H.

[1] We note that the distribution of percolation thresholds deviates slightly from a Gaussian even for random percolation [28].

4. Discussion

We have provided improved numerical estimates of percolation thresholds on self-affine lattices that approximate fBm. The results highlight important differences for percolation on self-affine surfaces compared to percolation on uncorrelated surfaces. These differences are consistent with previous studies by others [10–12,27].

Comparison of our results with Table 1 from Du et al. [11] shows an interpretation equivalent to p_c^{eith} or $\Re_0$. Similarly, a comparison with Fig. 6 from Schmittbuhl et al. [10] shows an interpretation equivalent to p_c^{spec} or $\Re_1$. Hence, the contrasting values between Du et al. [11] and Schmittbuhl et al. [10] can be explained when the various spanning rules are considered.

Given that the percolation thresholds depend strongly on the chosen spanning rule, one must consider which threshold to choose to evaluate scaling laws for percolation quantities [2], and if the scaling behavior is independent of the spanning rule. This work shows that definition of the percolation threshold should be considered with care. For application to common flow measurements performed on rock cores at a laboratory scale, percolation in a specified direction would be most appropriate. In this case, the introduction of correlations leads to a lower percolation threshold than observed on uncorrelated media, and hence a lower residual fluid saturation would be expected. These measurements are then used as input to reservoir simulators at scales of tens of meters – at these scales the spanning rule one should utilise is less clear. To obtain residual saturations close to values obtained in real rocks, this work will be extended to three dimensions.

Acknowledgements

SJM acknowledges the support of the Foundation of Chemical Research (SON) under the auspices of the Netherlands Research Organization (NWO). MAK is grateful to the Australian Research Council for financial support. We thank the A.N.U. Supercomputing Facility for allocations of computer time.

References

[1] R.G. Larson, L.E. Scriven, H.T. Davis, Nature 268 (1977) 409.
[2] M. Sahimi, Rev. Mod. Phys. 65 (1993) 1393.
[3] T. Hewett, SPE Annual Technical Conference and Exhibition, New Orleans, Society of Petroleum Engineers, Richardson, Texas, 1986, paper SPE 15 836.
[4] S. Painter, L. Paterson, Geophys. Res. Lett. 21 (1994) 2857.
[5] S. Painter, Water Resources Res. 32 (1996) 1183.
[6] K. Liu, P. Boult, S. Painter, L. Paterson, AAPG Bull. 80 (1996) 1850.
[7] H.A. Makse, S. Havlin, P.Ch. Ivanov, P.R. King, S. Prakash, H.E. Stanley, Physica A 233 (1996) 587.
[8] F.J. Molz, H.H. Liu, J. Szulga, Water Resources Res. 33 (1997) 2273.
[9] M.A. Knackstedt, A.P. Sheppard, W.V. Pinczewski, Phys. Rev. E 58 (1998) R6923.
[10] J. Schmittbuhl, J.-P. Vilotte, S. Roux, J. Phys. A 26 (1993) 6115.

[11] C. Du, C. Satik, Y.C. Yortsos, A.I.Ch.E. J. 42 (1996) 2392.
[12] M. Sahimi, S. Mukhopadhyay, Phys. Rev. E 54 (1996) 3870.
[13] G. Wagner, P. Meakin, J. Feder, T. Jøssang, Phys. Rev. E 55 (1997) 1698.
[14] L. Paterson, S. Painter, X. Zhang, W.V. Pinczewski, SPE Journal 3 (1998) 211.
[15] P.J. Reynolds, H.E. Stanley, W. Klein, Phys. Rev. B 21 (1980) 1223.
[16] J. Feder, Fractals, Plenum Press, New York, 1988.
[17] R.F. Voss, in: H.-O. Peitgen, D. Saupe (Eds.), The Science of Fractal Images, Springer, New York, 1988, 21–70 (Chapter 1).
[18] D. Saupe, in: H.-O. Peitgen, D. Saupe (Eds.), The Science of Fractal Images, Springer, New York, 1988, 71–136 (Chapter 2).
[19] R. Maeder, Math. J. 6 (1995) 38.
[20] Z.-M. Yin, J. Comput. Phys. 127 (1996) 66.
[21] R.M. Ziff, Phys. Rev. Lett. 69 (1992) 2670.
[22] J.-P. Hovi, A. Aharony, Phys. Rev. E 53 (1996) 235.
[23] J. Hoshen, R. Kopelman, Phys. Rev. B 14 (1976) 3438.
[24] D. Stauffer, A. Aharony, Introduction to Percolation Theory, 2nd Edition, Taylor & Francis, London, 1994.
[25] P. Grassberger, J. Phys. A 25 (1992) 5475.
[26] B.D. Hughes, Random Walks and Random Environments, Vol. 2, Clarendon Press, Oxford, 1996.
[27] Z. Olami, R. Zeitak, Phys. Rev. Lett. 76 (1996) 247.
[28] R.M. Ziff, Phys. Rev. Lett. 72 (1994) 1942.